A TECHNIQUE TO OPTIMIZE ISOCENTER CO-ORDINATE AND COLLIMATOR ANGLE IN RADIOSURGERY PLANNING FOR MULTIPLE BRAIN METASTASES

by

Hong Lam PHAM [1]***, Tien Manh PHAN*** [2]***, and Quang Trung PHAM*** [2,3*]

[1] Oncology Center, Military Hospital 103, Hanoi, Vietnam
[2] School of Engineering Physics, Ha Noi University of Sciences and Technology, Hanoi, Vietnam
[3] Radiation Oncology and Radiosurgery Department, 108 Military Central Hospital, Hanoi, Vietnam

Scientific paper
https://doi.org/10.2298/NTRP2501065P

Collimator angle optimization software CAOS was developed in Python and integrated with the Eclipse 13.6 platform to support stereotactic radiosurgery treatment planning. Twenty-five cases of multiple brain metastasis (10 with two lesions, 10 with three, and 5 with four) were planned using stereotactic radiosurgery in Eclipse 13.6, followed by optimization with CAOS. Eclipse uses a conventional method, while CAOS software first determines the isocenter co-ordinate and then optimizes the collimator angles. The CAOS-optimized plans exhibited significantly improved dosimetric outcomes in stereotactic radiosurgery planning. They reduced gradient index and gradient measure values for the tumor, decreased the mean normal brain volume receiving 12 Gy, and lowered the maximum dose to organs-at-risk, compared to Eclipse plans.

Key words: stereotactic radiosurgery, collimator angle optimization, Eclipse 13.6, normal brain tissue

INTRODUCTION

The brain metastasis treatment, particularly when multiple metastases are present, poses significant challenges in radiosurgery. Conventional methods such as surgery or stereotactic radiosurgery (SRS) by Gamma Knife, CyberKnife, TomoTherapy, and especially RapidArc with new modern linear accelerators, such as the TrueBeam STx system, are commonly employed [1-3]. In SRS planning, accurate isocenter determination and collimator angle optimization are crucial in these treatments to ensure the precise targeting of tumors while minimizing radiation exposure to healthy brain tissue. This is especially important in RapidArc, where dynamic modulation of radiation dose distribution is critical for effective treatment outcomes [4, 5].

While planning RapidArc for a single target on the TrueBeam STx with high-definition multi-leaf collimator (HD MLC) is relatively straightforward, treatment planning of multiple brain metastases presents significant complexities. Challenges include minimizing the dose to normal brain tissue, reducing side effects, and managing the *bridge dose* – the radiation dose delivered between two targets due to lack of shielding by collimator leaves. These issues can significantly impact the quality of the treatment plan and the patient's post-treatment quality of life. Current methods often rely on predetermined angular sections and collimator settings that may not be optimal for all patient geometries and overlook dynamic collimator rotation during delivery. This leads to inefficiencies and suboptimal treatment outcomes [4-7].

Several studies have attempted to address these issues through various optimization techniques. Kang *et al*. [8] developed an algorithm to optimize the treatment geometry of a volumetric modulated arc therapy (VMAT) plan by finding the minimal area of overlap of two lesions in the sinogram space. For different combinations of table and collimator angle, the overlap region will vary, once the minimum overlap area in the sinogram is found, the optimized table and collimator angle were determined. Wu *et al*. [9] conducted a study to minimize dose spill by identifying the smallest area where MLC leaves do not block radiation beams. They developed a projection summing optimization algorithm, which involved measuring the coordinates of outer boundary points of each lesion, projecting on a beam's eye view (BEV) plane, and calculating for each arc the ideal couch and collimator angles with the smallest overall open beam area. Pudsen *et al*. [10] also developed a collimator angle optimization algorithm using MATLAB to optimize collimator angles and monitor functions for multi-target

* Corresponding author, e-mail: qtphamhus@gmail.com

radiosurgery based on RapidArc when the lowest level of island blocking is achieved. Abuduxiku *et al*. [11] optimized the collimator angle by combining island blocking and parked gap, done with single-isocenter multi-lesion VMAT for stereotactic body radiation therapy (SBRT) of liver cancer; the collimator angle was determined based on the 2-D projection of targets on the BEV plane as a function of gantry and collimator angle. Despite these developments, issues remain in execution, including enhancing adjacent normal tissue coverage. This requires the simultaneous adjustment of the collimator angle, table angle, and the algorithms employed. These factors significantly influence the effectiveness of various optimization techniques. Our approach integrates the optimization of isocenter coordinates as input data to enhance the optimization of the collimator angle.

This study aims to demonstrate the effectiveness of the CAOS that has been developed to determine the isocenter co-ordinates and optimize collimator rotation for stereotactic radiosurgery of multiple brain metastases treated on the TrueBeam STx using the RapidArc technique on Eclipse 13.6. This software seeks to improve the accuracy and efficiency of RapidArc planning, thereby enhancing treatment outcomes and reducing exposure to healthy brain tissue.

METHODS

Software development

The CAOS is a software application designed to determine the isocenter and optimize the collimator angle for SRS plans on Eclipse 13.6. First, the software reads the necessary information, including the position and coordinates of the planning target volumes (PTV), the number of arcs, the gantry angles, and the couch rotation angles for each arc, directly from Eclipse 13.6. Upon acquiring this data , CAOS calculates the optimal isocenter for the SRS plan and susequently determines the collimator angle for each arc. To facilitate the calculation and analysis of the plan information, the software is developed in Python.

Isocenter co-ordinate determinate algorithm

Determining the treatment center coordinates for multiple treatment volumes in 3-D space (x, y, z), crucially involves minimizing the distance between the isocenter and the centers of these volumes across each coordinate axis.

Algorithm description

The isocenter of the SRS plan is represented as I (X_{iso}, Y_{iso}, Z_{iso}) calculated based on the projected coordinates of the treatment volumes onto the O_x, O_y, and O_z axes in the O_{xyz} space. The isocenter co-ordinate X_{iso}, Y_{iso}, and Z_{iso} is determined by calculating the mid-point of the furthest O_x, O_y, and O_z extents among all treatment volumes. The algorithm requires the number and the co-ordinates inputs of the treatment volume centers $PTV1\,(x_1, y_1, z_1)$, $PTV2\,(x_2, y_2, z_2)$, ..., $PTVn\,(x_n, y_n, z_n)$, it produces the optimized isocenter co-ordinates output $I\,(X_{iso}, Y_{iso}, Z_{iso})$. The isocenter co-ordinate determination algorithm is presented in fig. 1.

Collimator angle optimization algorithm

Figure 2 shows a collimator angle optimization algorithm for radiosurgery treatment planning. The gantry rotation is divided into control points 1° apart. For each specific gantry angle, the projection of lesions onto the BEV plane is represented in space. At each control point, the co-ordinates of the tumors will be altered based on the 3-D rotation matrix [12]. The total area of the MLC leaves blocking the radiation beams is calculated by summing the MLC area at each control point corresponding to the couch angle, gantry angle, and collimator angle. Then, the gantry and collimator angles with the largest total MLC area will be chosen as the optimization for that specific treatment arc.

STEP 1: Determining the origin axes

The x-axis (O_x) corresponds to the lateral direction, the y-axis (O_y) corresponds to the vertical direction, and the z-axis (O_z) corresponds to the longitudinal direction. The gantry rotates around the z-axis (O_z). The beam's eye view (BEV) surface remains consistently perpendicular to the y-axis (O_y) throughout gantry rotation. After determining the coordinates of the isocenter, denoted as $I\,(X_{iso}, Y_{iso}, Zi_{so})$, this value is used to define the isocenter for the SRS plan.

STEP 2: Determining the rotation matrix

Matrices represent the rotations of the gantry, couch, and collimator: Gantry (g) for the gantry, Table (t) for the table, and Collimator (c) for the collimator. When the gantry rotates around the z-axis by an angle (g°), this rotation is transformed into the new coordinate system O_{xyz}. The resulting rotation matrix is given by eq. (1)

$$\text{Gantry}\,(g) = \begin{bmatrix} \cos(g) & \sin(g) & 0 \\ -\sin(g) & \cos(g) & 0 \\ 0 & 0 & 1 \end{bmatrix} \quad (1)$$

When the couch rotates around the y-axis by an angle (t°), this rotation is transformed into the new coordinate system O_{xyz}. The resulting rotation matrix is given by eq. (2)

$$\text{Table}\,(t) = \begin{bmatrix} \cos(t) & 0 & -\sin(t) \\ 0 & 1 & 0 \\ \sin(t) & 0 & \cos(t) \end{bmatrix} \quad (2)$$

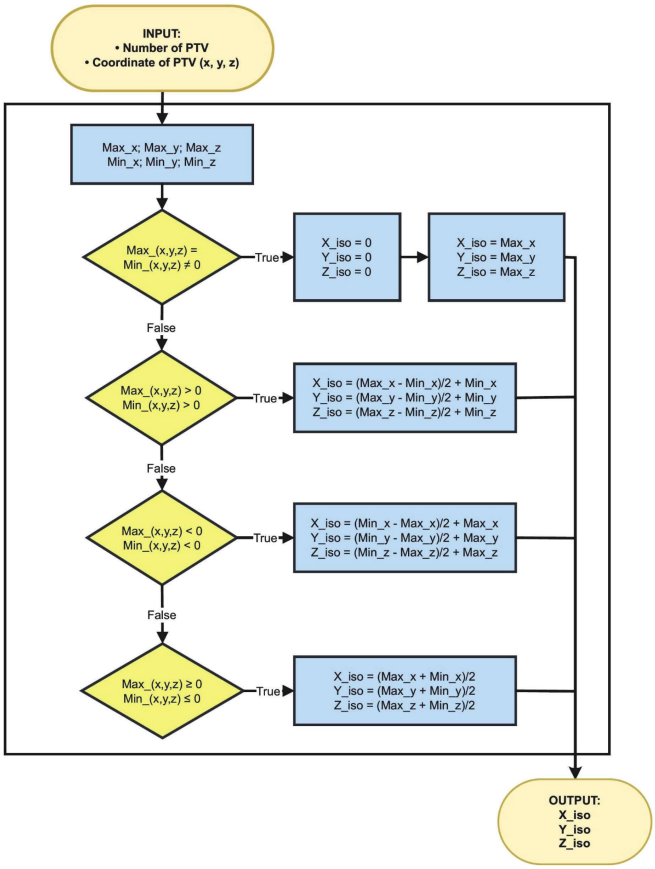

Figure 1. Isocenter co-ordinate determination algorithm for radiosurgery treatment planning

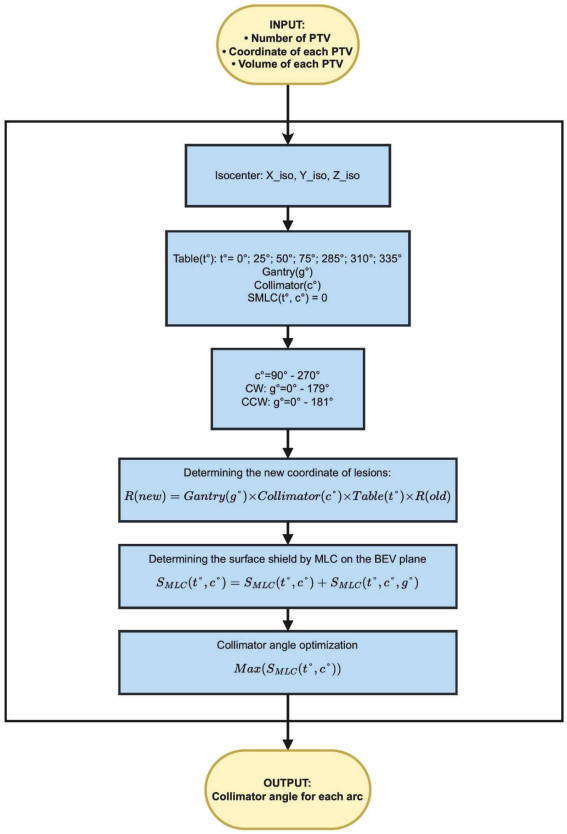

Figure 2. Collimator angle optimization algorithm for radiosurgery treatment planning

when the collimator rotates around the *y*-axis by an angle (c°), this rotation is transformed into the new co-ordinate system Oxyz. The resulting rotation matrix is given by eq. (3)

$$\text{Collimator}(c)=\begin{bmatrix}\cos(c) & 0 & -\sin(c)\\ 0 & 1 & 0\\ \sin(c) & 0 & \cos(c)\end{bmatrix} \quad (3)$$

STEP 3: Determining the new co-ordinate of lesions

The lesions are projected onto the BEV surface, providing a detailed view of the lesion surfaces in the BEV. As the gantry, couch, and table rotate, the lesions accordingly shift in position. The new co-ordinates of the lesions, *R*(new), are determined based on the previous co-ordinates, *R*(old), using the formula proposed by Wu *et al*. [9] as eq. (4)

$$R(new)=Gantry(g)\cdot Collimator(c)\cdot Table(t)\cdot R(old) \quad (4)$$

The co-ordinates of the lesion's border are used to calculate the MLC coverage on the *xOz* plane for any given gantry angle.

STEP 4: Determining the optimized collimator angle

When the collimator rotation is set to 0°, the movement direction of the MLC coincides with the *x*-axis on the *xOz* plane.

The plan BEV on the *xOz* is divided by pixel with the dimension by *n*·*m* is equal to the field size dimension, the maximum field size is 32 cm × 22 cm. Each pixel has a value of 1 cm^{-2}. If MLC shields a pixel, the system assigns it a value of 1. If MLC opens a pixel its value is 0. Equation (5) presents the shield of MLC on the *xOz* plan fig. 3.

$$\varepsilon(i,j)=\sum_{i=1}^{n}\sum_{j=1}^{m}h_{ij} \text{ with } h_{ij}=1 \text{ and } (n,m\in N^{*}) \quad (5)$$

The surface shield by MLC on the BEV plane is the sum of all pixels and is calculated

$$S_{\text{MLC}}=\varepsilon(n,m) \quad (6)$$

For simplicity, we assume that all lesions are spherical, each defined by a single center and a radius, determined by the lesion's volume. When the lesions are projected onto the BEV plane (*xOy*), the MLC aperture for each lesion is determined using a Boolean function [9]. The surface shield by MLC is presented by

$$S'_{\text{MLC}}=\varepsilon(n,m)-\varepsilon'(n,m) \quad (7)$$

The treatment volumes, characterized by their co-ordinates and integrals within Eclipse, are conceptualized as the centers of spheres with equivalent integrals. Their activity is assessed when projected onto the *xOz* plane of the BEV. For each fixed couch position and every combination of gantry and collimator angles, we calculate the cumulative activity of the treatment volumes on the *xOz* plane. The collimator angle varies incrementally from 90° to 270° in 1° steps (total 180°). Minimizing the total integral across all volumes on the BEV's surface indicates minimal MLC aperture and maximum MLC shielding. The optimal collimator angle is identified as the angle at which the total integral is minimized during gantry rotation from 0° to 180° in 1° increments.

For each collimator angle, the shielding surface by the MLC is calculated using an equation. The optimized collimator angle is the one that maximizes S'_{MLC}.

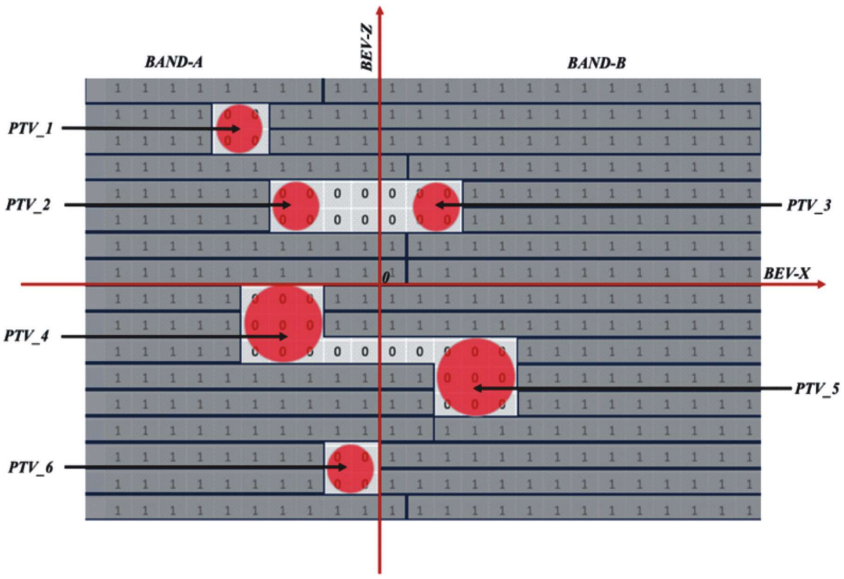

Figure 3. The lesions projected and MLC on the BEV surface *xOz*

The SRS planning and utilization of CAOS

A total of 25 cases of multi-metastasis brain tumors were used in the study, including 10 cases with two lesions, 10 cases with three lesions, and 5 cases with four lesions. A prescription dose of 18 Gy in a single fraction was applied and a non-coplanar RapidArc technique was utilized to plan. All cases were planned using collimator angles obtained from Eclipse v13.6 first, then replanned using collimator angles optimized by CAOS. The isocenter of the plan is the center of all lesions achieved from the CAOS. Each plan includes eight arcs, each corresponding to a different couch angle, with an energy of 6 MV FFF and a high dose rate of 1400 MU* per minute. The plans were optimized following the standard protocol to ensure quality using the configuration of TrueBeam STx linac (varian medical system).

The SRS plan evaluation and comparison

Table 1 presents the parameters used to evaluate dose distribution in the tumor. The evaluation of SRS plans incorporated various factors related to dose distribution in the PTV, including the conformity index (*CI*) [13, 14], gradient index (*GI*) [14], gradient measure (*GM*) [15], and dose tolerance for organ-at-risk (OAR) or the maximum dose (D_{max}). The *CI* quantifies the degree to which the prescribed dose conforms to the treatment volume; *GI* indicates dose reduction to healthy tissues surrounding the PTV; *GM* represents the difference in equivalent spherical radius calculated from the volume enclosed by the 50 % and 100 % dose lines, expressed in centimeters (cm). The most critical area to avoid excessive dose exposure is the normal brain tissue, particularly the mean normal brain volume receiving 12 Gy ($V12$), while also minimizing the bridge dose between lesions.

Table. 1 Parameters in evaluatin dose distribution on the tumor

Index	Formula	Ideal value
CI	$CI_{\mathrm{RTOG}} = \frac{V_{\mathrm{PIV}}}{PTV}$ (8)	$0.9 < CI < 1.2$
	$CI_{\mathrm{Paddick}} = \frac{(PTV_{\mathrm{PIV}})^2}{PTV \cdot V_{\mathrm{PIV}}}$ (9)	$CI = 1$
GI	$GI = \frac{V_{50}}{V_{\mathrm{PIV}}}$ (10)	$3.0 < GI < 5.0$
GM [cm]	$GI = R_{50\mathrm{PIV}} - R_{100\mathrm{PIV}}$ (11)	$GM = 0$

V_{PIV}: prescription isodose volume (cm^3), PTV: target volume (cm^3). PTV_{PIV}: volume of PTV receiving 100 % of prescription dose; V_{PIV}: volume covered by 100 % isolines. V_{50}: volume covered by 50 % of the prescription dose (cm^3). R_{50PIV}, R_{100PIV}: spherical radius calculated from the volume enclosed by the 50 % and 100 % dose lines (cm).

*MU – a unit used in radiation therapy (usually 1 cGy of radiation under standard conditions)

After obtaining optimized isocenter co-ordinates and collimator angles from CAOS, these parameters were applied to plan SRS in Eclipse 13.6. Simultaneously, we developed a separate plan in Eclipse, using its own optimized parameters. Plan evaluation for target coverage, dose spillage, and parameters for the OAR assessment follows guidelines such as RTOG 9005 [16], ICRU 91 [17], and AAPM 101 [18].

The SRS plans created using CAOS are compared to those generated with Eclipse v13.6 on target dose distribution and dose to normal brain tissue. The Wilcoxon signed-rank test was used to compare the differences between the two groups of treatment plans. $\overline{X} \pm s$ represents statistical results. Statistical significance was assessed using a p-value <0.05.

RESULTS AND DISCUSSION

Dosimetric parameters for tumors

Table 2 summarizes the mean values of the dosimetric parameters: *CI*, *GI*, and *GM* for both plan sets. All parameters met RTOG 9005 tolerances, with OAR doses within acceptable limits for single-fraction SRS plans based on RTOG 9005 and AAPM 101 recommendations.

The *CI* assesses dose alignment with the target volume. There was no difference in *CI* values between the CAOS and Eclipse v13.6 plans for all lesion groups. The CI_{RTOG} values were nearly identical for both methods across all groups, but the CI_{Paddick} value is quite low compared to the ideal value, indicating similar target conformity.

The *GI* measures the dose fall-off beyond the target, with lower values reflecting steeper dose gradients and better healthy tissue sparing. CAOS-optimized plans had significantly lower *GI* values than Eclipse on three- and four-lesion plans (with $p < 0.05$). The results suggest CAOS reduces the dose to surrounding tissues more effectively, minimizing side effects.

The *GM* gauges dose gradient sharpness, with lower values indicating steeper gradients. CAOS consistently reduced *GM* values, especially in all plan groups, pointing to sharper gradients and improved protection for adjacent tissues, as highlighted in studies by Wu *et al*. [9] and Pudsey *et al*. [10].

Dose distribution on normal tissues

In stereotactic radiosurgery, the $V12$ Gy index needs special attention because it is essential in predicting the risk of radiation-induced side effects, especially brain necrosis in radiosurgery patients treated for non arteriovenous malformations (AVM) [19].

Table 3 presents the mean normal brain volume receiving 12 Gy ($V12$). The CAOS-optimized plans consistently showed a lower mean normal brain vol-

Table 2. Comparison of the dosimetric parameters in tumors for plans with collimator angles optimized by CAOS and those from Eclipse 13.6

Dosimetric parameters		Plan with collimator angle from CAOS	Plan with collimator angle from Eclipse 13.6	*p*-value
Two lesions	CI_{RTOG}	1.11 ±0.01	1.11 ±0.01	0.14
	$CI_{Paddick}$	0.60 ±0.01	0.60 ±0.01	0.33
	GI	5.83 ±0.33	6.59 ±0.57	<0.05
	GM [cm]	0.52 ±0.02	0.56 ±0.03	<0.05
Three lesions	CI_{RTOG}	1.09 ±0.00	1.09 ±0.01	0.47
	$CI_{Paddick}$	0.60 ±0.00	0.60 ±0.00	0.14
	GI	6.21 ±0.20	6.43 ±0.18	≪0.05
	GM [cm]	0.63 ±0.01	0.64 ±0.01	<0.05
Four lesions	CI_{RTOG}	1.10 ±0.00	1.09 ±0.00	0.47
	$CI_{Paddick}$	0.60 ±0.08	0.60 ±0.01	0.14
	GI	6.61 ±0.09	6.78 ±0.10	<0.05
	GM [cm]	0.73 ±0.01	0.73 ±0.01	0.26

Table 3. Comparison of the mean value of the normal brain volume receiving 12 Gy for all plans with collimator angles optimized by CAOS and those from Eclipse 13.6

Number of lesions	*V*12 – CAOS [Gy]	*V*12 – Eclipse [Gy]	*p*-value
Two lesions	2.44 ±0.22	2.79 ±0.29	<0.05
Three lesions	3.89 ±0.18	4.06 ±0.17	<0.05
Four lesions	5.54 ±0.16	5.71 ±0.19	<0.05

ume receiving 12 Gy across all lesion groups (two, three, and four lesions showed a reduction of about 12.5 %, 4.2 %, and 3.0 % respectively), highlighting their effectiveness in sparing normal brain tissue. This reduction in *V*12 with CAOS-optimized plans indicates better sparing of normal brain tissue, potentially reducing the risk of cognitive and other side effects. These findings demonstrate that optimized planning techniques can significantly reduce the exposure of normal brain tissue to high radiation doses.

The D_{max} distributed to the organ-at-risk should be as small as possible, which minimizes damage and complications for patients and improves treatment effectiveness and quality of life. Table 4 shows that most of the D_{max} doses of OAR on the CAOS plan (D_{max}-CAOS) are lower than those calculated by Eclipse (CAOS-Eclipse) in all groups of 2 to 4 lesions. Especially, left and right eyeballs in all CAOS plans receive lower doses than in Eclipse plans. This result is particularly significant because the lens dose tolerance is very low and should be considered carefully when planning treatment [20]. All D_{max} dose values on organ-at-risk were less than the tolerable dose. Although the comparisons do not show statistically significant differences, they partly show the effectiveness of CAOS.

Typically, collimator angles are optimized and obtained from Eclipse 13.6, however, this approach often results in dose distributions with bridge doses between lesions and elevated dose levels to normal brain tissue. It can be noticed that CAOS significantly enhances the quality of SRS plans by improving the dose distribution on the tumor while reducing the dose to normal brain tissue. The CAOS-optimized plans showed consistently lower *GI* and *GM* values, reflecting sharper dose gradients and better conformity across lesion types. This sharper dose fall-off minimizes radiation to healthy tissue, an advantage particularly evident in multi-lesion cases where conventional methods may struggle. Our findings align with studies like Tham *et al*. [21], confirming that automated optimization can significantly improve dose conformity.

The lower *GI* and *GM* values, combined with reduced *V*12 volumes and lower doses on other organs at risk, demonstrated that CAOS could effectively optimize treatment plans, providing better protection for healthy tissues without compromising target coverage. These improvements are particularly notable in plans with multiple lesions, where achieving dose distribution and normal tissue sparing are more challenging. These findings suggest that CAOS can enhance the precision and safety of SRS treatments for patients with multiple brain metastases.

The CAOS integrates with Eclipse 13.6 for an efficient RapidArc planning process, reducing manual work and enhancing precision. This study highlights CAOS's ability to refine SRS planning for complex cases by optimizing dose distribution while ensuring normal tissue sparing. However, CAOS currently optimizes only collimator angles thus limiting further refinement in complex cases. Additionally, the study's sample size is small, with only up to four lesions per case, which limits generalizability. For enhanced treatment precision, future improvements should incorporate gantry and couch angles optimization, testing on a larger patient cohort to encompass diverse lesion configurations, and ensure broader effectiveness.

Table 4. Comparison of maximum dose D_{max} on OAR

OAR		D_{max} – CAOS [cGy]	D_{max} – Eclipse [cGy]	*p*-value
Two lesions	Left lens	36.10 ±5.47	37.58 ±6.60	0.31
	Right lens	40.89 ±10.31	34.46 ±11.28	0.24
	Brainstem	89.37 ±14.49	101.00 ±18.05	0.08
	Chiasm	83.22 ±13.89	90.75 ±17.26	0.09
	Left eyeball	79.54 ±18.23	82.53 ±19.21	0.09
	Right eyeball	69.42 ±17.15	70.79 ±19.78	0.44
	Left optic nerve	68.81 ±14.39	72.41 ±14.86	0.26
	Right optic nerve	51.96 ±9.89	56.42 ±12.67	0.16
Three lesions	Left lens	50.35 ±5.10	55.39 ±6.65	0.14
	Right lens	52.70 ±8.48	54.80 ±8.42	0.29
	Brainstem	140.66 ±12.71	153.61 ±9.58	0.11
	Chiasm	128.72 ±12.27	131.96 ±16.17	0.34
	Left eyeball	116.86 ±19.65	120.02 ±20.27	0.33
	Right eyeball	90.43 ±13.12	98.36 ±16.53	0.27
	Left optic nerve	108.50 ±15.18	108.73 ±17.93	0.49
	Right optic nerve	93.46 ±10.43	84.41 ±10.05	0.09
Four lesions	Left lens	67.16 ±5.52	68.86 ±6.87	0.40
	Right lens	72.48 ±11.45	86.56 ±13.59	0.08
	Brainstem	197.54 ±20.60	176.06 ±19.69	0.18
	Chiasm	177.50 ±17.70	170.08 ±6.10	0.33
	Left eyeball	153.92 ±20.60	169.04 ±24.71	0.10
	Right eyeball	128.00 ±14.91	134.96 ±19.81	0.21
	Left optic nerve	136.68 ±14.67	143.24 ±20.07	0.26
	Right optic nerve	143.32 ±24.37	137.82 ±19.45	0.30

CONCLUSION

In conclusion, the CAOS has demonstrated significant improvements in determining the isocenter coordinates and the optimization of collimator angles for SRS planning using RapidArc. The CAOS plans exhibited reduced *GI* and *GM* values for the tumor, together with diminished *V*12 volumes and D_{max} for organs-at-risk, in comparison to the Eclipse plans. The enhanced dose distribution and reduced normal brain dose achieved with CAOS optimization have important clinical implications for improving patient outcomes and minimizing treatment-related side effects. These findings support the integration of CAOS into routine clinical practice as a valuable tool for advanced radiosurgery planning.

AUTHORS' CONTRIBUTIONS

H. L. Pham and T. M. Phan authored the manuscript, collected, and analyzed the data, and developed the software. Q. T. Pham conceived the study, supervised the research, and reviewed and edited the manuscript.

ACKNOWLEDGMENT

We express our gratitude to the Department of Radiation Oncology and Radiosurgery at the 108 Military Central Hospital for their support of this work.

ORCID NO

H. L. Pham: 0009-0009-7549-9719
Q. T. Pham: 0009-0003-4941-0836

REFERENCES

[1] Timmerman, R. D., Park, C., Kavanagh, B. D., The North American Experience with Stereotactic Body Radiation Therapy in Non-Small Cell Lung Cancer, *Journal of Thoracic Oncology, 2* (2007), 7, pp. S101-S112
[2] Vesper, J., *et al.*, Current Concepts in Stereotactic Radiosurgery-A Neurosurgical and Radiooncological Point of View, *European Journal of Medical Research, 14* (2009), Mar., pp. 93-101
[3] Nieder, C., Grosu, A. L., Gaspar, L. E., Stereotactic Radiosurgery (SRS) for Brain Metastases: A Systematic Review, *Radiation Oncology, 9* (2014), July, pp. 1-9
[4] Minniti, G., *et al.*, Stereotactic Radiosurgery for Brain Metastases: Analysis of Outcome and Risk of Brain Radionecrosis, *Radiation Oncology, 6* (2011), May, pp. 1-9
[5] Christ, S. M., *et al*., Stereotactic Radiosurgery for Brain Metastases from Malignant Melanoma, *Surgical Neurology International, 6* (2015), Suppl 12, p. S355
[6] Warsi, N. M., *et al*., The Role of Stereotactic Radiosurgery in the Management of Brain Metastases From a Health-Economic Perspective: a systematic Review, *Neurosurgery, 87* (2020), 3, pp. 484-497
[7] Lippitz, B., *et al*., Stereotactic Radiosurgery in the Treatment of Brain Metastases: the Current Evidence, *Cancer Treatment Reviews, 40* (2014), 1, pp. 48-59

[8] Kang, J., *et al.*, A method for Optimizing LINAC Treatment Geometry for Volumetric Modulated Arc Therapy of Multiple Brain Metastases, *Medical Physics, 37* (2010), 8, pp. 4146-4154
[9] Wu, Q., *et al*., Optimization of Treatment Geometry to Reduce Normal Brain Dose in Radiosurgery of Multiple Brain Metastases with Single-Isocenter Volumetric Modulated Arc Therapy, *Scientific Reports, 6* (2016), 1, 34511
[10] Pudsey, L. M., *et al*., The Use of Collimator Angle Optimization and Jaw Tracking for VMAT-based single-isocenter multiple-target stereotactic radiosurgery for up to six targets in the Varian Eclipse treatment planning system, *Journal of Applied Clinical Medical Physics, 22* (2021), 9, pp. 171-182
[11] Abuduxiku, M., *et al*., Optimization of Collimator Angle Combined Island Blocking with Parked Gap Achieves Superior Normal Tissue Sparing in SBRT Planning of Multiple Liver Lesions, *Journal of Applied Clinical Medical Physics, 25* (2024), 6, p. e14267
[12] Sarabandi, S., *et al*., On Closed-Form Formulas for the 3-D Nearest Rotation Matrix Problem, *IEEE Transactions on Robotics, 36* (2020), 4, pp. 1333-1339
[13] Shaw, E., *et al.*, Radiation Therapy Oncology Group: Radiosurgery Quality Assurance Guidelines, *International Journal of Radiation Oncology* Biology* Physics, 27* (1993), 5, pp. 1231-1239
[14] Paddick, I., Lippitz, B., A Simple Dose Gradient Measurement Tool to Complement the Conformity Index, *Journal of Neurosurgery, 105* (2006), Supplement, pp. 194-201
[15] Hoffman, D., Lung Stereotactic Body Radiation Therapy (SBRT) Dose Gradient and PTV Volume: a Retrospective Multi-Center Analysis, *Radiation Oncology, 14* (2019), Sept., pp. 1-7
[16] Shaw, E., *et al.*, Single Dose Radiosurgical Treatment of Recurrent Previously Irradiated Primary Brain Tumors and Brain Metastases: Final Report of RTOG Protocol 90-05, *International Journal of Radiation Oncology* Biology* Physics, 47* (2000), 2, pp. 291-298
[17] Seuntjens, J., Prescribing, Recording, and Reporting of Stereotactic Treatments With Small Photon Beams, ICRU report 91, 2017, IAEA-CN-250, pp. 273-274
[18] Benedict S. H., *et al*., Stereotactic Body Radiation Therapy: the Report of AAPM Task Group 101, *Medical Physics, 37* (2010), 8, pp. 4078-4101
[19] Korytko, T., *et al*., 12 Gy Gamma Knife Radiosurgical Volume is a Predictor for Radiation Necrosis in Non-AVM Intracranial Tumors, *International Journal of Radiation Oncology* Biology* Physics, 64* (2006), 2, pp. 419-424
[20] Samac, J., *et al*., Assessment of Occupational Eye Lens Exposure During Image-Guided Orthopedic Procedures, *Nucl Technol Radiat, 38* (2023), 3, pp. 202-207
[21] Tham, B. Z., *et al*., Plan Assessment Metrics for Dose Painting in Stereotactic Radiosurgery, *Advances in Radiation Oncology, 8* (2023), 6, 101281

Received on March 28, 2025
Accepted on June 5, 2025

Хонг Лам ФАМ, Тин Мањ ФАН, Кванг Трунг ФАМ

ОПТИМИЗОВАЊЕ ИЗОЦЕНТАРСКЕ КООРДИНАТЕ И УГЛА КОЛИМАТОРА У ПЛАНИРАЊУ РАДИОХИРУРГИЈЕ ВИШЕСТРУКИХ МОЖДАНИХ МЕТАСТАЗА

Софтвер за оптимизовање угла колиматора (CAOS) развијен је на Пајтону и интегрисан са платформом Eclipse 13.6 како би се подржало планирање стереотактичке радиохирургије. Двадесетпет случаја вишеструких метастаза на мозгу (десет са две, десет са три и пет са четири лезије) планирано је, најпре коришћењем стереотактичке радиохирургије у Eclipse-у 13.6, а затим помоћу CAOS-а. Eclipse је користио конвенционалну методу, док CAOS софтвер одређује координату изоцентра, а затим оптимизује углове колиматора. Планови оптимизовани помоћу CAOS-а показали су значајно побољшане дозиметријских исхода за планирање стереотактичке радиохирургије смањујући вредности градијентног индекса и мере градијента за тумор, заједно са смањењем средње нормалне запремине мозга која прима дозу од 12 Gy и смањењем максималне дозе за ризичне органе, у поређењу са Eclipse плановима.

Кључне речи: стереотактичка радиохирургија, оптимизовање угла колиматора, Eclipse 13.6, нормално мождано ткиво